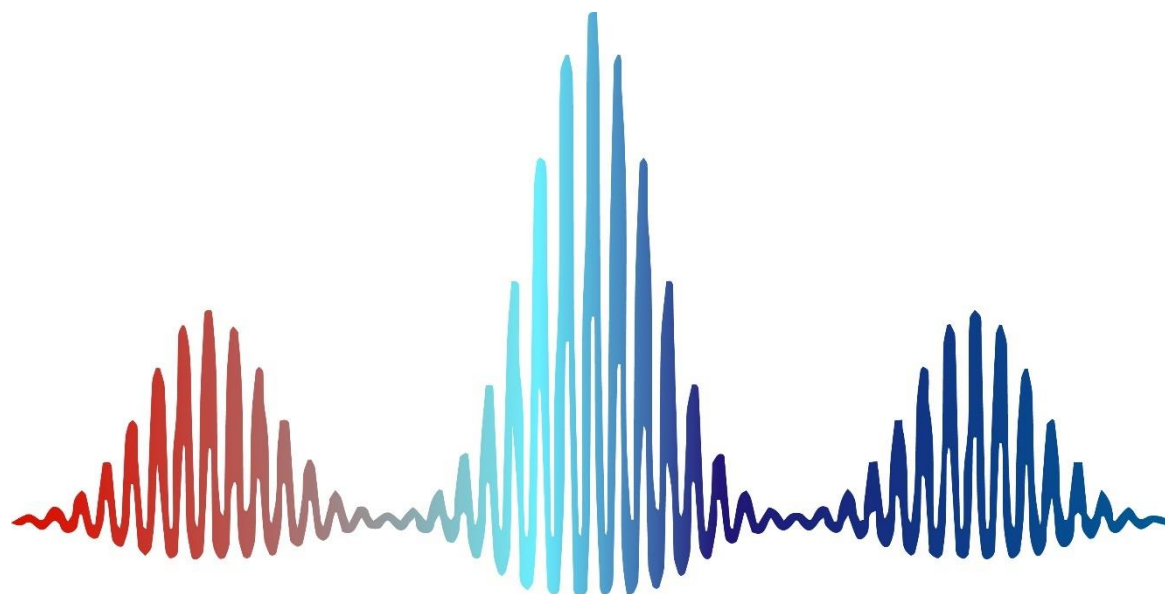


А.О. Набилкова, Е.Н. Опарин, А.Н. Цыпкин

**LABORATORY ASSIGNMENTS FOR
THE COURSES OF "FEMTOSECOND OPTICS
AND FEMTOTECHNOLOGY"
AND "TERAHERTZ TECHNOLOGIES"
(Experimental part)**



**Санкт-Петербург
2022**

**МИНИСТЕРСТВО ОБРАЗОВАНИЯ И НАУКИ
РОССИЙСКОЙ ФЕДЕРАЦИИ**

УНИВЕРСИТЕТ ИТМО

А.О. Набилкова, Е.Н. Опарин, А.Н. Цыпкин

**LABORATORY ASSIGNMENTS FOR
THE COURSES OF "FEMTOSECOND OPTICS
AND FEMTOTECHNOLOGY"
AND "TERAHERTZ TECHNOLOGIES"
(Experimental part)**

УЧЕБНО-МЕТОДИЧЕСКОЕ ПОСОБИЕ

**РЕКОМЕНДОВАНО К ИСПОЛЬЗОВАНИЮ
В УНИВЕРСИТЕТЕ ИТМО**

по направлению подготовки 12.04.03 Фотоника и оптоинформатика
в качестве учебно-методического пособия для реализации основных
профессиональных образовательных программ высшего образования
магистратуры

 **УНИВЕРСИТЕТ ИТМО**

Санкт-Петербург

2022

А.О. Набилкова, Е.Н. Опарин, А.Н. Цыпкин, «Femtosecond optics and femtotechnology» и «Terahertz Technologies». – СПб: Университет ИТМО, 2022. – 39 с.

Рецензент(ы):

Петров Николай Владимирович, доктор физико-математических наук, доцент, доцент (квалификационная категория "ординарный доцент") факультета фотоники и оптоинформатики, Университета ИТМО.

В пособии представлены учебно-методические материалы лабораторного практикума по дисциплине «Femtosecond optics and femtotechnology» и «Terahertz Technologies». Представлены теоретические сведения, методические указания и порядок выполнения лабораторных работ. Освещаются основополагающие вопросы, связанные с оптикой фемтосекундных и терагерцовых импульсов, в частности, практическое их применение для исследования линейных и нелинейных свойств различных материалов этого раздела оптики. Также продемонстрированы экспериментальные способы определения длительности изучаемых сверхкоротких оптических импульсов. Предназначено для бакалавров и магистров, обучающихся по направлению подготовки 12.04.03 «Фотоника и оптоинформатика».



Университет ИТМО – ведущий вуз России в области информационных и фотонных технологий, один из немногих российских вузов, получивших в 2009 году статус национального исследовательского университета. С 2013 года Университет ИТМО – участник программы повышения конкурентоспособности российских университетов среди ведущих мировых научно-образовательных центров, известной как проект «5 в 100». Цель Университета ИТМО – становление исследовательского университета мирового уровня, предпринимательского по типу, ориентированного на интернационализацию всех направлений деятельности.

©Университет ИТМО, 2022

А.О. Набилкова, Е.Н. Опарин, А.Н. Цыпкин, 2022

Table of contents

Laboratory assignment №1

SECOND HARMONIC GENERATION BY FEMTO-SECOND LASER RADIATION IN A UNIAXIAL NONLINEAR CRYSTAL	4
---	---

Laboratory assignment №2

MEASUREMENT OF ULTRASHORT PULSE DURATION BY AUTOCORRELATION TECHNIQUES	14
---	----

Laboratory assignment №3

STUDY OF NONLINEAR PROPERTIES OF OPTICAL MATERIALS USING THE Z-SCAN METHOD	23
---	----

Laboratory assignment №4

TERAHERTZ TIME-DOMAIN SPECTROSCOPY	30
--	----

Laboratory assignment №1

SECOND HARMONIC GENERATION BY FEMTO-SECOND LASER RADIATION IN A UNIAXIAL NONLINEAR CRYSTAL

Work objective:

To investigate the process of generating the second optical harmonic in a uniaxial nonlinear crystal illuminated with femtosecond radiation.

Tasks:

1. To study the principles of radiation frequency conversion in media with second-order nonlinear susceptibility;
2. To determine the optimal conditions for generating the second harmonic in a uniaxial β -BBO crystal illuminated by femtosecond radiation;
3. To measure the dependence of the second harmonic power on the pump radiation power, as well as on the crystal position. Analyze the spectra of the first and the generated second harmonics.

SOME THEORY

In classical optics, all electromagnetic phenomena are described by Maxwell's Equations (1.1):

$$\begin{aligned}(\nabla, \mathbf{D}) &= 4\pi\rho, & [\nabla, \mathbf{E}] &= -\frac{1}{c} \frac{\partial \mathbf{B}}{\partial t}, \\(\nabla, \mathbf{B}) &= 0, & [\nabla, \mathbf{H}] &= \frac{1}{c} \frac{\partial \mathbf{D}}{\partial t} + \frac{4\pi}{c} \mathbf{j},\end{aligned}\tag{1.1}$$

Solution of the Maxwell's Equations is impossible without introducing constitutive equations connecting the fields \mathbf{E} and \mathbf{D} , \mathbf{H} and \mathbf{B} with equations (1.1):

$$\begin{aligned}\mathbf{D} &= \mathbf{E} + 4\pi\mathbf{P}, \\ \mathbf{H} &= \mathbf{B} - 4\pi\mathbf{M},\end{aligned}\tag{1.2}$$

where \mathbf{P} and \mathbf{M} are the polarization and magnetization vectors of the medium (the density of its electric and magnetic moment). The induction of the magnetic moment of the medium is rather inertial, and at frequencies characteristic of

optical radiation (about 10^{-15} Hz), the magnetization does not have time to occur, that is, we can assume that $\mathbf{M} = 0$, and $\mathbf{H} = \mathbf{B}$.

The polarization of the medium is proportional to the electric field strength, and this dependence can be represented as a series over the field:

$$\begin{aligned}\mathbf{P} &= \chi^{(1)}\mathbf{E} + \chi^{(2)}\mathbf{E}\mathbf{E} + \chi^{(3)}\mathbf{E}\mathbf{E}^2 + \dots = \mathbf{P}^{(1)} + \mathbf{P}^{(2)} + \mathbf{P}^{(3)} + \dots = \\ &= \mathbf{P}^{(1)} + \mathbf{P}^{NL},\end{aligned}\quad (1.3)$$

where $\chi^{(n)}$ is the n-th order dielectric susceptibility of the medium.

Taking into account the above considerations (equations (1.1) – (1.3)), the Maxwell's Equations will take the form:

$$\begin{aligned}(\nabla, \mathbf{D}) &= -4\pi(\nabla, \mathbf{P}^{NL}), & [\nabla, \mathbf{E}] &= -\frac{1}{c} \frac{\partial \mathbf{B}}{\partial t}, \\ (\nabla, \mathbf{B}) &= 0, & [\nabla, \mathbf{H}] &= \frac{1}{c} \frac{\partial \mathbf{D}}{\partial t} + \frac{4\pi}{c} \frac{\partial \mathbf{P}^{NL}}{\partial t}.\end{aligned}\quad (1.4)$$

From equation (1.4) we get the wave equation:

$$-\Delta \mathbf{E} + \frac{\varepsilon}{c^2} \frac{\partial^2 \mathbf{E}}{\partial t^2} = -\frac{4\pi}{c^2} \frac{\partial^2 \mathbf{P}^{NL}}{\partial t^2}.\quad (1.5)$$

This equation (1.5) shows that an electromagnetic wave with its intensity excites a wave of nonlinear polarization in the medium, which, in turn, becomes a source of electromagnetic waves (in the general case, at other frequencies too). Typical values of the dielectric conductivity of media are given in Table 1.1:

Table 1.1 — Typical values of the dielectric conductivity of media

	CGS	SI
χ^1	1	1
χ^2	$10^{-9} - 10^{-8}$	$10^{-12} - 10^{-11}$ m/V
χ^3	$10^{-14} - 10^{-15}$	$10^{-22} - 10^{-21}$ m^2/V^2

The second-order susceptibility values are translated from one system of units to other using the formula: $\chi^2[SI] = \frac{4\pi}{3 \times 10^4} \chi^2[CGS]$.

For this assignment, we will consider the effects arising due to the presence of a second-order nonlinear susceptibility in the medium, which can only be a

medium without central symmetry possess. That is, we assume $P^{NL} = \chi^{(2)}EE$.

To describe second-order effects, we generally represent the input field as two waves of different frequencies:

$$E(t) = \frac{1}{2} [A_1 e^{i\omega_1 t} + A_2 e^{i\omega_2 t} + c. c.]. \quad (1.6)$$

Then the second-order nonlinear polarization P^{NL} from equation (1.3) takes the form:

$$\begin{aligned} P^{NL} &= \chi^{(2)} E^2 = \\ &= \frac{1}{4} \chi^{(2)} [2(|A_1|^2 + |A_2|^2) + A_1 e^{i2\omega_1 t} + A_2 e^{i2\omega_2 t} \\ &\quad + 2A_1 A_2 e^{i(\omega_1 + \omega_2)t} + 2A_1 A_2 e^{i(\omega_1 - \omega_2)t} + c. c.]. \end{aligned} \quad (1.7)$$

In this case, the polarization wave is excited at twice the frequencies of $2\omega_1$ and $2\omega_2$, the difference $(\omega_1 + \omega_2)$ and the total $(\omega_1 - \omega_2)$, as well as the zero frequency.

To simplify, however, we can assume that a nonlinear medium is affected by a monochromatic field with a frequency ω , so equation (1.7) takes the form:

$$\begin{aligned} E(t) &= E_1 \cos \omega t, \\ P^{NL} &= \frac{1}{2} \chi^{(2)} E_1^2 + \frac{1}{2} \chi^{(2)} E_1^2 \cos 2\omega t. \end{aligned} \quad (1.8)$$

Expression (1.8) means that the polarization will have a constant component of $0.5\chi^{(2)}E_1^2$ and a variable of $0.5\chi^{(2)}E_1^2 \cos 2\omega t$ at twice the frequency 2ω . The first term corresponds to a process called optical rectification, and the second term corresponds to second harmonic generation.

Take a closer look at the second harmonic generation (SHG) process. To do this, we discard the constant term and substitute the expression for the nonlinear polarization of the medium in the wave equation, which we write for a plane monochromatic wave propagating along the z axis:

$$\frac{d^2 E_2}{dt^2} + \frac{4\omega^2}{c^2} \varepsilon(2\omega) E_2 = \frac{8\pi\omega^2}{c^2} E_1^2 \cos(2\omega t - 2k_1 z), \quad (1.9)$$

here E_1 is the field of the electromagnetic wave at the fundamental frequency, and E_2 at the doubled frequency.

Solving the differential equation (1.9), we obtain:

$$E_2 \propto E_1^2 \frac{\sin(\Delta kz/2)}{\Delta kz/2} = E_1^2 \cdot \text{sinc}(\Delta kz/2), \quad (1.10)$$

where $\Delta k = k_2 - 2k_1$ is the detuning of the pump (with wave vector k_1) and second harmonic (with wave vector k_2) wave vectors. Thus, the harmonic intensity is easily found:

$$I_2 \propto I_1^2 \frac{\sin^2(\Delta kz/2)}{(\Delta kz/2)^2} = I_1^2 \cdot \text{sinc}^2(\Delta kz/2). \quad (1.11)$$

When the phase detuning is nonzero, the intensity of the second harmonic oscillates as the radiation propagates in the medium, that is, there is a recurrent transfer of energy from the first harmonic to the second and back. In this case, the distance at which the second harmonic reaches its maximum intensity is called the coherence length: $z_c = \frac{\pi}{\Delta k}$.

In practice, the observation of this effect is complicated by the impossibility to quickly change the thickness of a nonlinear medium. Instead, however, it is possible to change the screen thickness. To do this, a plane-parallel sample is rotated around an axis perpendicular to the beam and parallel to the optical axis of the crystal. The effective thickness of the medium in this case is $d \cos \theta$, where d is the thickness of the sample, and θ is the angle between the normal to the sample surface and the direction of beam propagation. The pattern of dependence of the second harmonic intensity on the rotation angle observed in this case is a sequence of maxima known as Maker's beats [3], that phenomena is shown on Figure 1.1.

The efficiency of SHG can be significantly increased if the conditions of equality of Δk to zero or, in other words, the phase synchronism conditions are satisfied. In this case, the phase velocities of light waves at the fundamental frequency and at the harmonic frequency are equal, and phase equality is achieved between the harmonic generated by certain given atoms and the wave that has come from the previous section of the medium. As a result, constructive interference of these waves occurs, and the harmonic amplitude monotonically increases as the radiation propagates. It seems clear that the intensity of the radiation generated in this case grows quadratically: $I_2 \propto I_1^2 z^2$. Those process are illustrated on Figure 1.2.

The condition of equality of the phase velocities of electromagnetic waves requires the equality of the refractive indices of the medium for these waves. However, this is hindered by the normal dispersion of most media, in which the refractive index increases with the increasing light frequency.

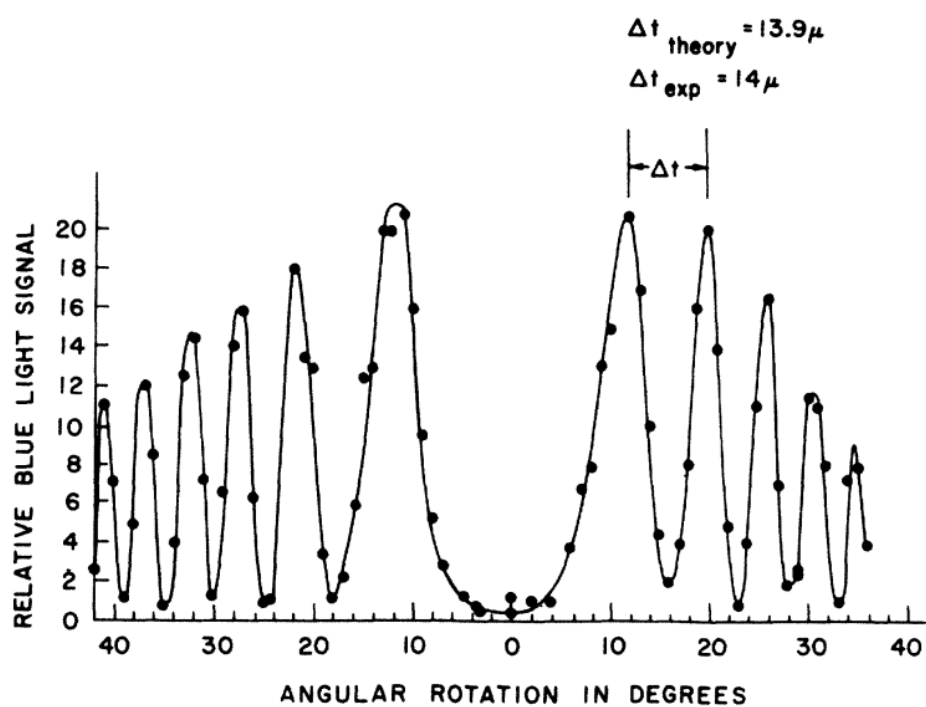


Figure 1.1 – Change in the second harmonic intensity on the crystal rotation angle. The axis of rotation is perpendicular to the beam and parallel to the optical axis of the crystal [3]

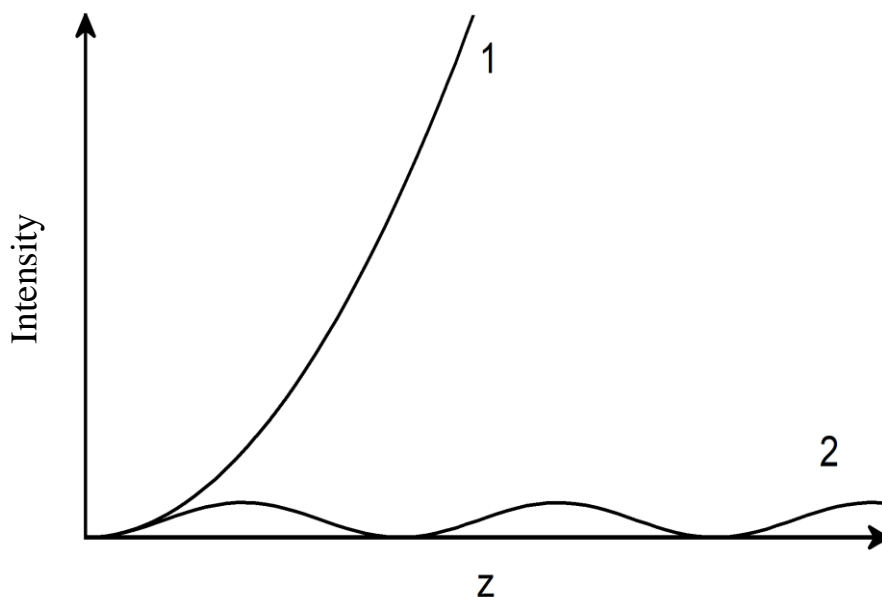


Figure 1.2 – Change in the second harmonic radiation intensity along the crystal: 1 - the synchronism condition is met, 2 - the synchronism condition is not met

This problem can be circumvented by using anisotropic crystals for SHG. In a negative uniaxial crystal, the phase velocities of waves at the fundamental and doubled frequencies can be equal if these waves have different polarizations: the pump is usually an ordinary wave, and the harmonic is an extraordinary one. The refractive index surfaces for this case are shown in Figure 1.3. It shows that for a certain direction in the crystal, the ellipsoid of the refractive index of the extraordinary wave intersects with the sphere of the refractive index of the ordinary one. This direction is called the synchronism direction, and this type of synchronization is denoted by *ooe*.

Regarding the optics of anisotropic media, we can show that *ooe*-synchronism angle θ_c^{ooe} in a uniaxial nonlinear crystal is calculated based on the expressions [4]:

$$tg^2 \theta_c^{ooe} = \frac{1 - U}{W - 1}, \quad U = \left(\frac{2A}{B} \right)^2, \quad W = \left(\frac{2A}{C} \right)^2, \\ A = \frac{n_{01}}{\lambda_1}, \quad B = \frac{n_{02}}{\lambda_2}, \quad C = \frac{n_{e2}}{\lambda_2}. \quad (1.12)$$

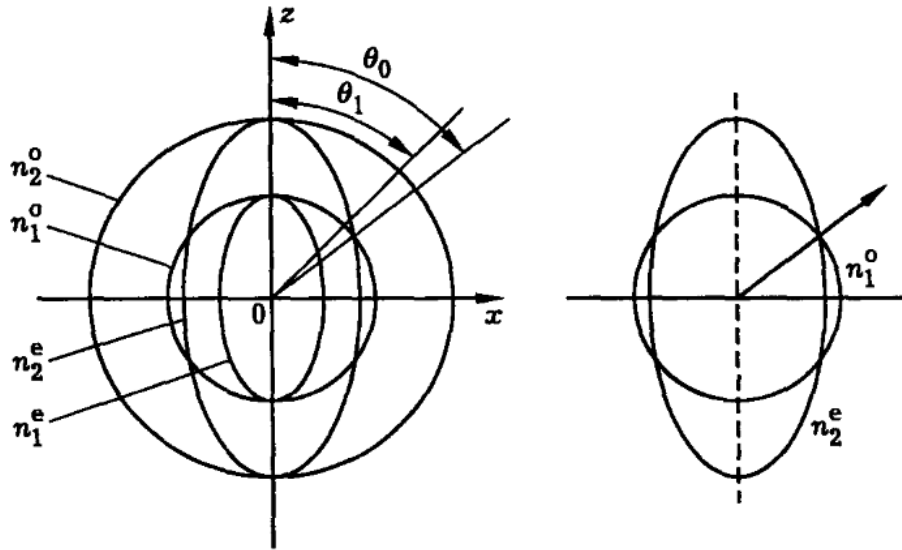


Figure 1.3 - Conditions of phase synchronization in a KDP crystal. On the left, sections of the surfaces of refractive indices are shown: a sphere for an ordinary wave (n^o) and an ellipsoid for an extraordinary (n^e) in a KDP crystal for the frequency of a ruby laser (index "1") and its second harmonic (index "2"). At an angle of θ_0 to the optical axis of the crystal, the circle n_1^o intersects with the ellipsoid n_2^e . This is the direction of synchronism. The figure on right one shows the direction of phase synchronism for in a negative uniaxial crystal ($n_1^o = n_2^e$).

The refractive indices of the nonlinear β -BBO crystal studied in this assignment for the wavelength of the laser used can be calculated based on its dispersion dependence (λ - in microns):

$$\begin{aligned} n_o^2 &= 2,7405 + \frac{0,0184}{\lambda^2 - 0,0179} - 0,0155\lambda^2, \\ n_e^2 &= 2,3730 + \frac{0,0128}{\lambda^2 - 0,0156} - 0,0044\lambda^2. \end{aligned} \quad (1.13)$$

Knowing the synchronization angle is important for practical work. Thus, in the manufacture of second-harmonic crystal generators used in science and technology, the crystal cut-off plane perpendicular to the direction of synchronism is chosen. This makes it possible to further install crystals normally to optical radiation, which minimizes the losses and beam displacement caused by Fresnel reflection.

For this assignment we will use femtosecond laser radiation as a pump. The use of ultrashort pulses to generate the second harmonic introduces a number of specific limitations, which are associated with the group delay of the pulses relative to each other, as well as with their dispersion spreading.

The first effect is that due to the dependence of the group velocity on the wavelength, the pulse of the second harmonic shifts in time relative to the pulse at the fundamental frequency as the radiation propagates in a nonlinear crystal. The second harmonic pulse can be both ahead of and behind the pump pulse. In this case, radiation is generated over the entire length of the crystal, and because of this, the second harmonic pulse is broadened in time relative to the initial pulse at the fundamental frequency.

To estimate the effect of the group delay effect, you should enter the parameter L_{qs} – the length of the group velocity variance, also referred to as the quasi-static interaction length:

$$L_{qs} = \tau_p \left(\frac{1}{u_{1-1}} - \frac{1}{u_{2-1}} \right)^{-1}, \quad (1.14)$$

where τ_p is the pump pulse duration, u_1 and u_2 are the group pulse velocities at the first and second harmonic frequencies. L_{qs} is equal to the length of the medium on which the pump pulses and the generated radiation diverge in space by a distance equal to the pulse length. If the crystal length is less than the quasi-static length, then the group delay effect can be ignored. In addition, under certain conditions, the difference in group speeds can tend to zero ($u_1 = u_2$) – this situation is called group synchronization.

Another effect occurs – that of dispersion spreading of pulses. In fact, due to the dispersion of the group velocity, ultrashort pump pulses and second harmonics are subject to time broadening, in varying degrees. To assess the implications effect of this effect, we introduce the characteristic length of the dispersion blur:

$$L_{dis} = \frac{\tau_p^2}{GVD}. \quad (1.15)$$

Here, GVD is the group velocity variance (see [5]). The effect has to be taken into account if the length of the medium is greater than this value, which is essential for pulses the duration of which is less than about 100 fs.

DESCRIPTION OF THE EXPERIMENTAL SETUP

An Ytterbium femtosecond laser with a central wavelength of 1050 nm is used as the radiation source. The characteristic integrated radiation power is 2.5 W, the pulse repetition rate is 70 MHz, and the pulse duration is 100 fs. The second harmonic is generated in a uniaxial negative crystal of barium beta-borate (β -BBO) with a thickness of 300 microns, designed to work with pump radiation with a central wavelength of 800 nm.

This experimental setup is shown in Figure 1.4. The laser radiation is focused into the β -BBO crystal by L_1 lens, after which it is again collimated by L_2 . Neutral glasses NG filter is used for general attenuation of the laser beam, and the BGG filter is used for the isolation of second-harmonic radiation at a wavelength of 525 nm. Radiation characterization is performed using a power meter PM and spectrometer S . Half-wave plate $\lambda/2$ and Glan-Taylor prism G curves are used to change the power of laser radiation.

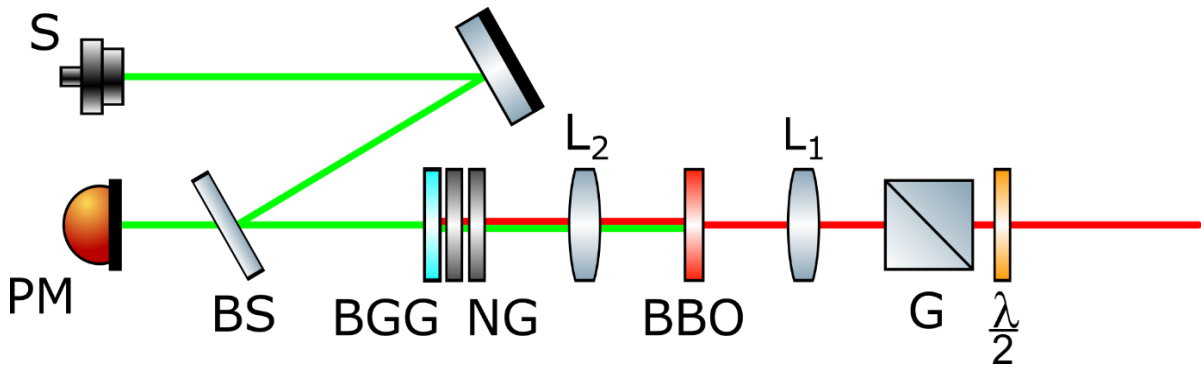


Figure 1.4 – Experimental setup

INSTRUCTIONS

1. Calculate the synchronization angle β -BBO for the central radiation wavelength of the laser used in operation (1050 nm) and for the wavelength that the crystal is designed to work with (800 nm). Determine at what angle to the optical beam it is necessary to position the crystal for the greatest efficiency of the SHG process.
2. By rotating the crystal in the frame, estimate the angular dependences of the second harmonic power. Identify the positions with the highest conversion efficiency.
3. By setting the crystal according to the direction of synchronism, investigate the dependence of the second harmonic radiation power on the pump power. The power change is carried out by turning the radiation polarization with a half-wave plate installed in front of the polarizer (Glan-Taylor prism).
4. To do this, enter the power values of the second harmonic at different angles of rotation of the half-wave plate in the table below. Measurements are to be made from the position $\lambda/2$ corresponding to the maximum power to the position corresponding to the minimum in 2-degree increments. Then remove the crystal from the optical circuit and repeat the measurement for pump radiation.

$\varphi_{\lambda/2}$	P_{ω}	$P_{2\omega}$
...

5. Using a spectrometer, register the spectra of laser radiation and the generated second harmonic. Determine their half-width.
6. Calculate the length of the quasi-discrete interaction and the dispersion length in the β -BBO crystal for pulses with durations of 30, 100, and 250 fs. Draw conclusions about the limitations on the crystal thickness for the cases under consideration.

SELF-ASSESSMENT QUESTIONS

1. In what substances is it possible to observe the generation of the second harmonic? What crystallographic and optical properties are they supposed to have?
2. What are the conditions for efficient second harmonic generation? How can they be implemented?
3. Based on the condition for efficient generation of the second harmonic, draw a conclusion about the ratio of the widths of the pump and harmonic emission spectra.
4. Is it possible that the group velocities of the pump pulses and the second harmonic are equal to each other? What it would lead to?

References

- [1] Akhmanov S. A., Nikitin S. Yu. Physical optics. Textbook – - 2004.
- [2] Shen I. R. Principles of nonlinear optics. – Ripoll Classic, 1989.
- [3] Maker P. D. et al. Effects of dispersion and focusing on the production of optical harmonics // *Physical Review Letters*. – 1962. – T. 8. – №. 1. – C. 21.
- [4] Gurzadyan G. G., Dmitriev V. G., David N. N. Nonlinear optical crystals: Properties and application in quantum electronics: Handbook. - Radio and Communication, 1991.
- [5] Optical constants of BaB₂O₄ (Barium borate, BBO). URL: <https://refractiveindex.info/?shelf=main&book=BaB2O4&page=Eim-erl-o>

Laboratory assignment №2

MEASUREMENT OF ULTRASHORT PULSE DURATION BY AUTOCORRELATION TECHNIQUES

Work objective:

Measure the durations of ultrashort pulses by autocorrelation techniques.

Tasks:

1. To get acquainted with the main autocorrelation techniques of measuring the duration of ultrashort pulses;
2. To determine the duration of femtosecond pulses using the intensity autocorrelation technique;
3. To determine the duration of femtosecond pulses by autocorrelation interferometry.

SOME THEORY

Autocorrelation of intensity

Measurement of the autocorrelation intensity function was the first attempt to study the time distribution of the intensity of an ultrashort pulse. In the 1960s, it became clear that there was no "shorter" standard with which to measure the duration of ultrashort pulses. When performing autocorrelation measurements, the pulse itself is used to determine its own duration. This method is based on the interaction of two pulses obtained by splitting the input radiation into two identical parts, one of which is shifted relative to the other by an arbitrary time delay τ . There are two cases, both collinear and a noncollinear intensity autocorrelation methods. In both cases, the superposition of two beams occurs in some rapidly reacting nonlinear optical medium, such as, for example, a second harmonic crystal generator (SHG) (see Figure 2.1 (noncollinear case)). The SHG crystal, along with collinear beams of the second harmonic, emits a third noncollinear "signal" beam between the first two harmonics. Its intensity is defined as follows:

$$E_{sig}^{SHG}(t, \tau) \propto E(t)E(t - \tau), \quad (2.1)$$

where τ is the delay between pulses.

The intensity of this radiation is proportional to the product of the intensities of the two input pulses:

$$I_{sig}^{SHG}(t, \tau) \propto I(t)I(t - \tau). \quad (2.2)$$

The speed of the detectors is not enough to directly measure the time dependence of the intensity. Instead, the autocorrelation function of intensity is measured:

$$A^{(2)}(\tau) = \int_{-\infty}^{+\infty} I(t)I(t - \tau)dt. \quad (2.3)$$

The superscript (2) means that this autocorrelation function has a second order. It is also possible to obtain a first (without using SHG) order autocorrelation and third order (based on the generation of third harmonics in media, with prevailing cubic nonlinearity), but these aspects will not be covered in this tutorial.

Figure 2.1 shows an example of an experimental scheme for measuring the autocorrelation function of the intensities of two ultrashort pulses. The input pulse is split into two by means of a beam splitter. By mechanical slide, a variable delay of one of the received pulses relative to the other is provided, after which both pulses overlap in the SHG crystal at a small angle. The detector registers the intensity of the generated noncollinear second harmonic at different values of the time delay, which makes it possible to obtain an autocorrelation curve. Other second-order nonlinear optical effects, such as two-photon fluorescence and two-photon absorption, can also produce autocorrelation when using a similar geometry.

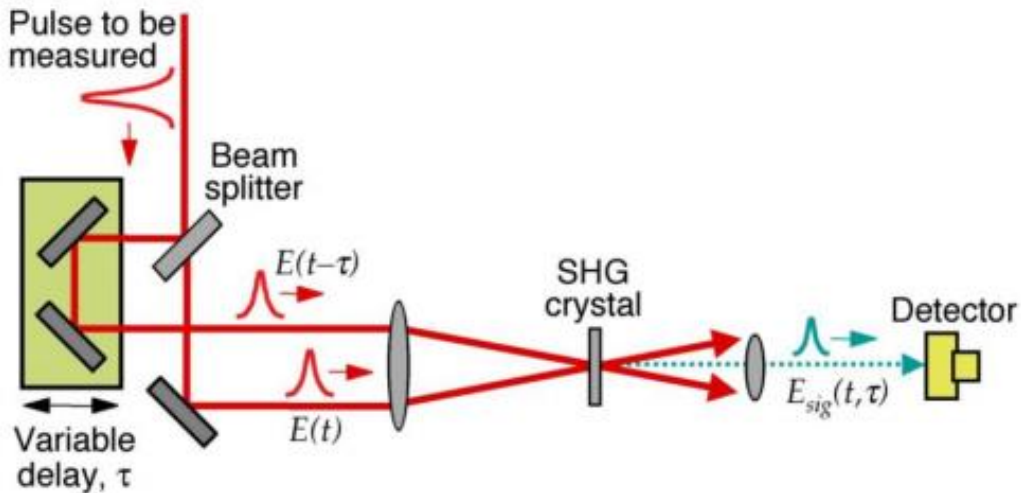


Figure 2.1 - Scheme of an intensity autocorrelator based on the generation of a noncollinear second harmonic

Figure 2.2 shows some examples of autocorrelation functions for pulse shapes. Note that autocorrelation measurements lose details of the pulse shape. This leads to the fact that all the reduced pulses have similar autocorrelation functions. In addition, intensity autocorrelation in intensity does not provide any information about the pulse phase.

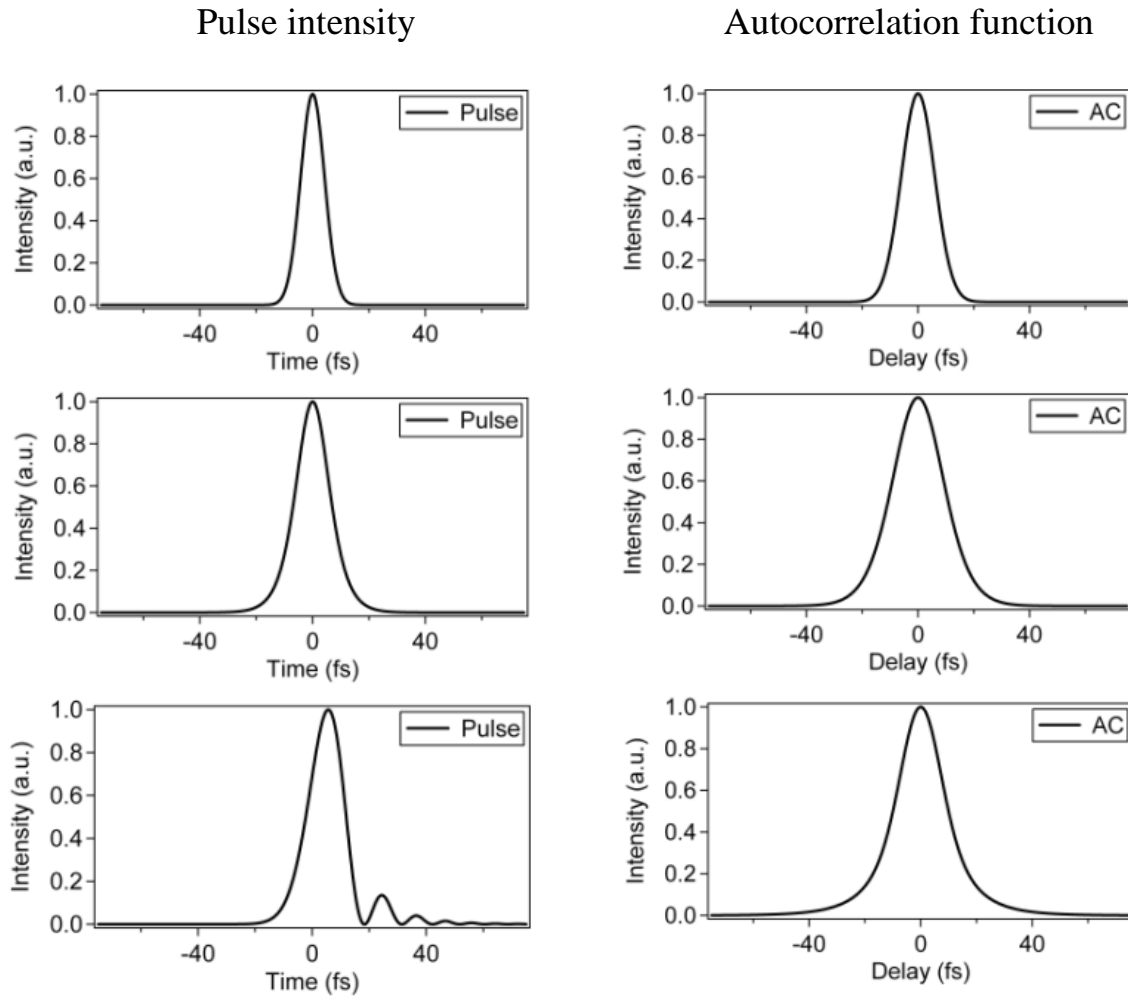


Figure 2.2 - Examples of theoretically defined pulse intensity distributions and their autocorrelation functions. Top row: A Gaussian pulse with a duration of 10 fs. Middle row: 7 fs sech² pulse. Bottom row: pulse subject to phase modulation

It is important to note that the ratio of the width of the autocorrelation function at half-height (FWHM) to the pulse duration is different for various laser pulse shapes (see Table 2.1). In this assignment, we assume that the momentum has the form of a hyperbolic secant. That is, to determine the laser pulse duration, the

measured value of the width of the autocorrelation function must be multiplied by 0.648.

Table 2.1 - Ratio of the width of the autocorrelation function at half-height (FWHM) to the pulse duration

Pulse type	$\Delta A/\Delta t$
Gaussian	1,414
$\text{sech}^2(t)$	1,543

Autocorrelation interferometry

Autocorrelation interferometry is a method for studying pulses, which makes it possible to obtain information on the characteristics both directly related to autocorrelation and the spectral composition of radiation. This method is also often referred to as phase-sensitive autocorrelation and FRAC (fringe-resolved autocorrelation).

This method is based on the Michelson interferometer, where splitting into two beams from one source in mutually perpendicular directions is carried out by a beam-splitting plate. A typical diagram of this interferometer used to measure the autocorrelation function of a laser pulse is shown in Figure 2.3. Detection of the interferometer output signal is based on the nonlinear effect of two-photon conductivity in a semiconductor.

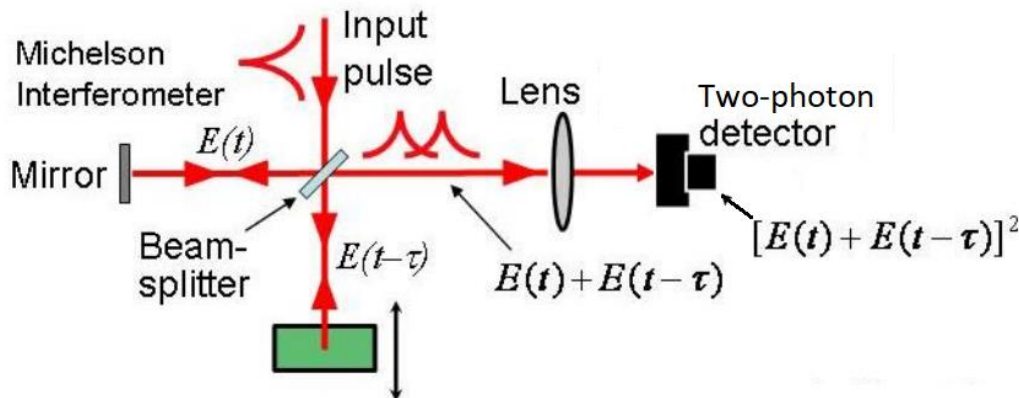


Figure 2.3 - Experimental setup for autocorrelation interferometry

Expression for the FRAC signal:

$$\begin{aligned}
 I_{FRAC}(\tau) &= \int_{-\infty}^{+\infty} |[E(t) + E(t - \tau)]|^2 dt = \\
 &= \int_{-\infty}^{+\infty} |E^2(t) + 2E(t)E(t - \tau) + E^2(t - \tau)|^2 dt. \quad (2.4)
 \end{aligned}$$

Note that if the terms $E^2(t)$ and $E^2(t - \tau)$ were removed from the above expression, only the cross term $2E(t)E(t - \tau)$ would be preserved, so we would get the usual expression for the autocorrelation of intensity. The new terms, integrals of $E^2(t)$ and $E^2(t - \tau)$, and their interaction, both with each other and with the cross term, allow us to obtain additional information that is not available in the usual autocorrelation function.

We also note a curious feature that makes it possible to verify the accuracy of the measurements performed. With zero delay between interfering pulses, the following applies:

$$I_{FRAC}(\tau = 0) = 16 \int E^4(t) dt, \quad (2.5)$$

and when the delay time tends to infinity:

$$I_{FRAC}(\tau = \infty) = 2 \int E^4(t) dt. \quad (2.6)$$

Therefore, the contrast of this method is always equal to 8. If a different value is obtained in the experiment, then an error occurred during the measurements.

Figure 2.4 shows some examples of FRAC curves, corresponding to different ultrashort pulse shapes.

Note that the accompanying pulses, due to the presence of phase modulation in the signal, introduce changes in the side "wings" of the FRAC curve. That is, the method of autocorrelation interferometry allows obtaining some information about the details of the time waveform, which is impossible when measuring autocorrelation in intensity. However, this information is quite limited. It is possible to fully investigate the phase of the signal using more sophisticated methods – frequency-resolved optical gating (FROG) or spectral-phase interferometry for direct restoration of the electric field (SPIDER).

DESCRIPTION OF THE EXPERIMENTAL SETUP

In this assignment, the pulse duration of an Ytterbium femtosecond laser with a central wavelength of 1050 nm is characterized. The typical integrated radiation power is 2.5 W, and the pulse repetition rate is 70 MHz. A noncollinear second harmonic is generated in a uniaxial negative crystal of barium beta-borate (β -BBO) with a thickness of 300 microns.

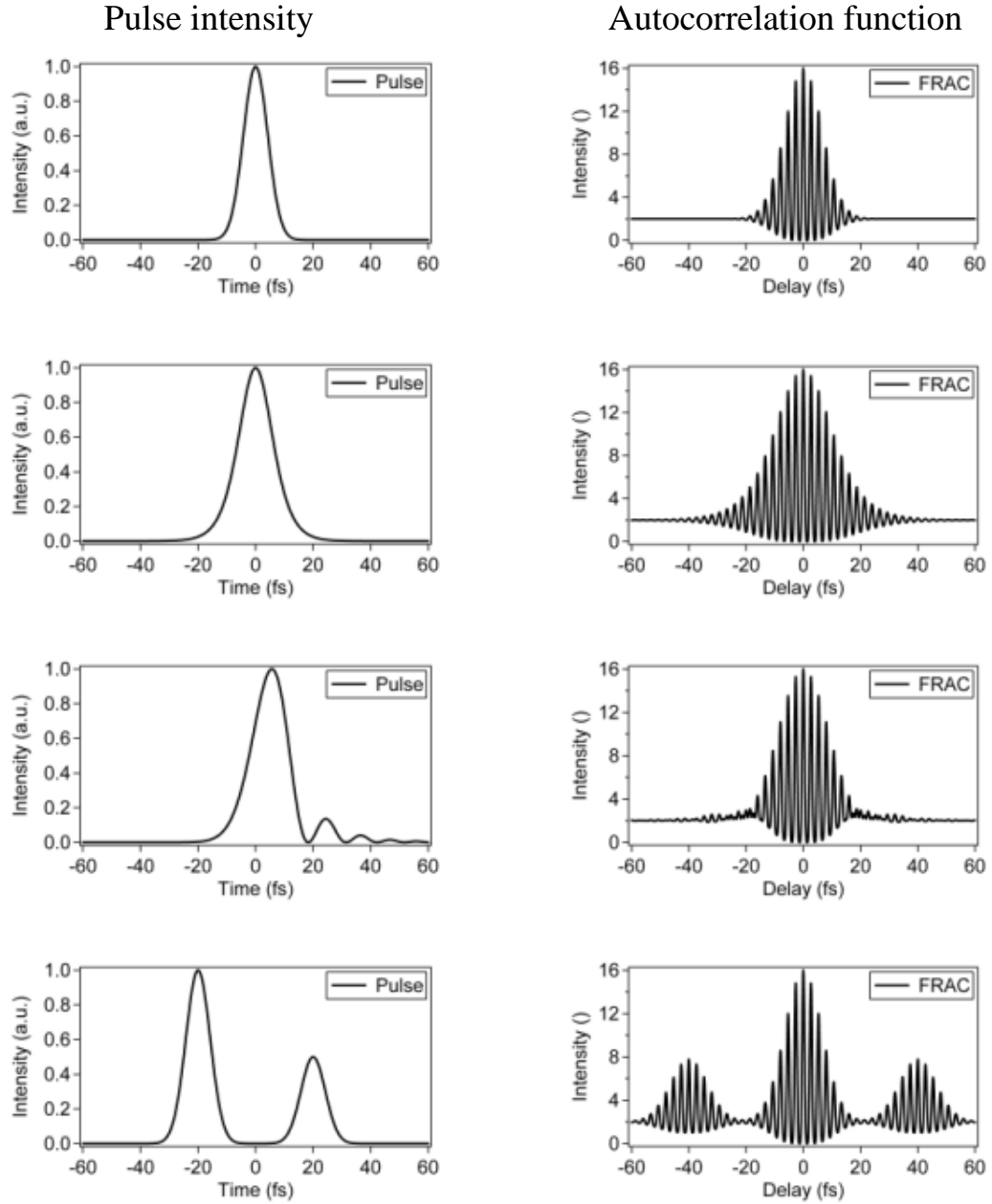


Figure 2.4 - Pulses and their corresponding FRAC curves. Top row: A Gaussian pulse with a duration of 10 fs. Second row: 7-fs sech^2 pulse. Third line: pulse subject to phase modulation. Fourth row: double pulse.

1 part

The experimental setup used in the first part of this paper is shown in Figure 2.5. Laser radiation is split into two beams of the same power by a beam splitter BS. One of the beams is reflected from two mirrors mounted on a mechanical slide that delays one of the pulses relative to the other.

The other beam, passing through a similar rigidly fixed pair of mirrors, hits the *SHG* crystal, where it intersects with the first one. The power of the generated noncollinear second harmonic is recorded by the power meter *PM*.

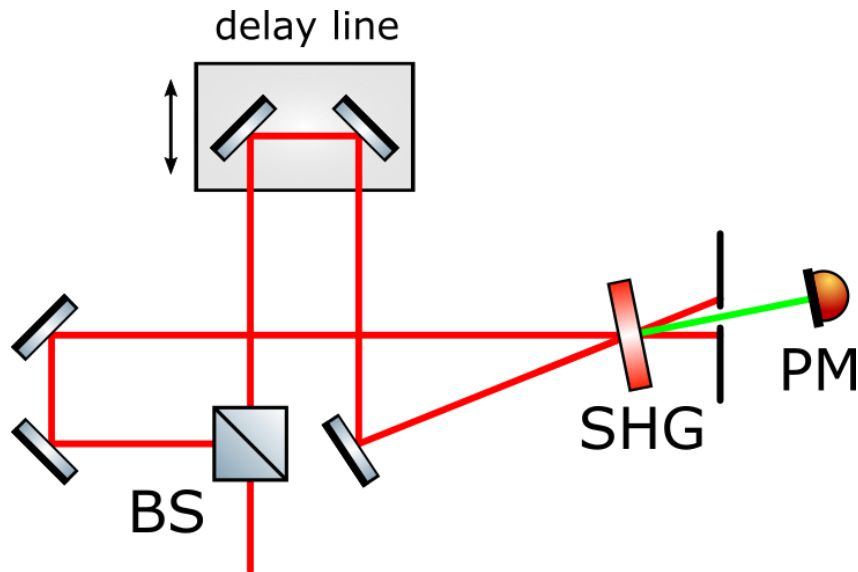


Figure 2.5 – Scheme of the experimental setup of the intensity autocorrelator

2 part

The second part of the work is performed using AA-20DD, the Avesta-Project scanning autocorrelator. The device is designed following the principle of a Michelson interferometer - the nonlinear effect of two-photon conductivity in a semiconductor is used to detect the autocorrelation function. The path of the rays is shown in Figure 2.6. The device is ready for operation and does not require any additional adjustment.

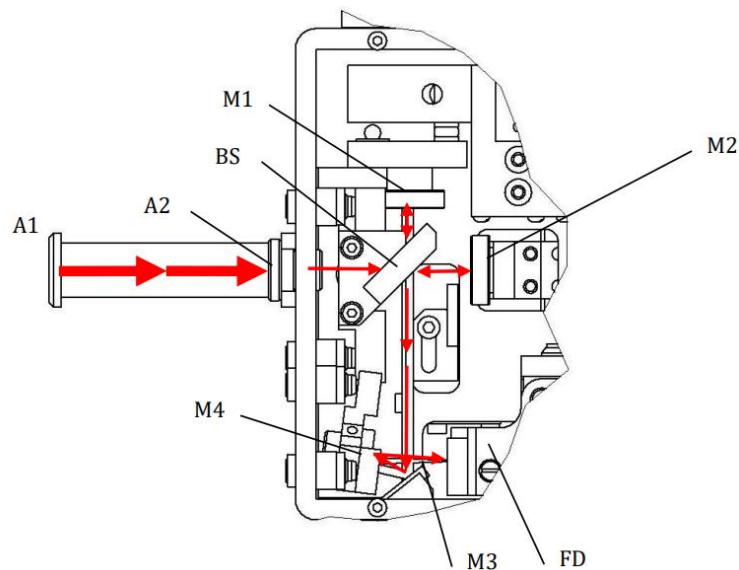


Figure 2.6 – Ray path in the AA-20DD scanning autocorrelation

INSTRUCTIONS

1 part

1. Perform primary alignment of the optical autocorrelator based on the generation of a noncollinear second harmonic according to the scheme, shown in Figure 2.5. Make sure that the laser beam is positioned at the same height on all sections of the circuit.
2. Achieve the overlap in the space of beams incident on the SHG crystal. This can be done from the visible glare on the front face of the crystal.
3. Observing the crystal generation of a noncollinear second harmonic (NSHG), allow the femtosecond pulses to overlap in time. The maximum intensity in the beam considered corresponds to the case when there is no delay between the pulses.
4. Install a light filter behind the crystal that removes pump radiation.
5. Position the detector head so that only the noncollinear SH beam falls on it.
6. At the signal from the detector, repeat the alignment of the pump beams in space. Maximize the NSG signal.
7. By shifting the displacement, vary the delay between pump pulses. Investigate the change in the intensity of NSG at different delays. This dependence corresponds to the autocorrelation function of the intensity of the pulse under study.
8. Determine the full width at half-height (FWHM) of the autocorrelation function. Draw conclusions about the pulse duration, assuming that its shape corresponds to a hyperbolic secant.

2 part

1. Make sure that the laser power used in the measurement does not exceed 20 mW! If this value is exceeded, the detection system of the autocorrelator may be damaged.
2. By means of two diaphragms and two mirrors, introduce radiation into the scanning autocorrelator AA-20DD: using the first mirror along the beam path, achieve a uniform illumination of the first diaphragm, and use the second mirror for the second diaphragm.
3. Observe on the computer screen the autocorrelation interferogram and the autocorrelation function of the intensity of the femtosecond pulse under study using the Irtac software.
4. Save the received dependencies to a text file. Plot them in an external software package (for example, Origin).

5. Determine the half-widths of autocorrelation functions. Draw conclusions about the pulse duration, assuming that its shape corresponds to a hyperbolic secant.
6. Compare the values obtained in the first and the second parts of this assignment.

SELF-ASSESSMENT QUESTIONS

1. What factors hinder the direct measurement of the ultrashort pulses duration? What are the techniques of indirect measurement?
2. Give some examples of the effects which provide the possibility of carrying out autocorrelation measurements? Summarize them.
3. Do autocorrelation methods of measurement make it possible to draw a conclusion about the phase modulation of the pulses studied? How can one make a conclusion whether it is presence or not?

References

- [1] Trebino R. Frequency-Resolved Optical Gating: The Measurement of Ultrashort Laser Pulses: The Measurement of Ultrashort Laser Pulses. – Springer Science & Business Media, 2000.
- [2] Intensity Autocorrelation – Swamp Optics Tutorial, 2015
- [3] Interferometric Autocorrelation – Swamp Optics Tutorial, 2015

Laboratory assignment №3

STUDY OF NONLINEAR PROPERTIES OF OPTICAL MATERIALS USING THE Z-SCAN METHOD

Work objective:

Get to know the principles of studying the nonlinear properties of materials using the z-scanning technique, as well as measuring the nonlinear coefficient of the refractive index of certain substances.

Tasks:

1. To learn the basics and features of the z-scan method;
2. To get z-scan curves for open-and closed-aperture installation configurations;
3. To calculate the nonlinear refractive index coefficient of the substances studied.

SOME THEORY

As discussed in previous laboratory assignments (on the second harmonic generation process, for example), the polarization of the medium induced by radiation can be represented as a series of:

$$\begin{aligned} \mathbf{P} &= \chi^{(1)}\mathbf{E} + \chi^{(2)}\mathbf{E}\mathbf{E} + \chi^{(3)}\mathbf{E}\mathbf{E}^2 + \dots = \mathbf{P}^{(1)} + \mathbf{P}^{(2)} + \mathbf{P}^{(3)} + \dots = \\ &= \mathbf{P}^{(1)} + \mathbf{P}^{NL}, \end{aligned} \quad (3.1)$$

where $\chi^{(n)}$ is the n-th order dielectric susceptibility of the medium.

In this assignment, we will consider the effects associated with the presence of a third-order nonlinear susceptibility in the medium, namely, the phenomenon of radiation self-focusing. It should be noted that the presence of nonzero $\chi^{(3)}$ is characteristic of any media, i.e., the observation of third-order nonlinear effects does not require any special conditions other than adequate radiation intensity.

We assume $P = \chi^{(1)}E + \chi^{(3)}E^3$. Whilst, the refractive index of the medium is determined by the formulas: $D = E + 4\pi P = \epsilon E = n^2 E$, whence

$$n = \sqrt{1 + \frac{4\pi P}{E}}. \quad (3.2)$$

Given the presence and the negligible of the nonlinear term, we obtain:

$$n = n_0 + \frac{2\pi}{n_0} \chi^{(3)} E^2, \quad (3.3)$$

where $n_0 = \sqrt{1 + 4\pi\chi^{(1)}}$. Move from the square of the radiation field strength to its intensity - I :

$$n = n_0 + n_2 I, \quad (3.4)$$

where $n_2 = \frac{16\pi^2}{n_0 c} \chi^{(3)}$. Here n_0 is the linear refractive index of the medium.

The expression obtained shows that in media with cubic nonlinearity, the refractive index depends on the light intensity. This effect leads to self-action of light waves, in particular, to self-focusing of the light beam, phase self-regulation of the pulse, bistability of a resonator filled with a nonlinear medium, and other effects.

Let us take a closer look at the self-focusing effect. The effects associated with a nonlinear addition to the refractive index are of particular interest for limited light beams. Here, an optical effect occurs, which can be referred to as nonlinear refraction. Indeed, in the field of a limited light beam, the initially homogeneous optical medium becomes inhomogeneous due to nonlinearity – the refractive index of the medium is determined by the distribution of the intensity of the propagating wave. The character of nonlinear refraction is determined by the sign of n_2 . In a medium with $n_2 > 0$, the region of maximum light intensity is optically denser. Obviously, in this case, nonlinear refraction leads to a concentration of energy – the peripheral rays are deflected into the region, where the field is maximal. This effect is called self-focusing of the light beam. An important factor that distinguishes the self-focusing effect from other nonlinear optical processes is its "avalanche" nature. Indeed, even a slight increase in intensity over a small section of the light beam in a medium with $n_2 > 0$ leads to a concentration of rays in this region, and consequently to an additional increase in intensity – this fact enhances the effect of self-focusing.

The value n_2 , which has the dimension of the inverse light intensity, is a convenient characteristic of the cubic nonlinearity of the medium. One of the ways to determine it is the z-scan method proposed by Mansoor Sheik-Bahae. It measures the transmission of a focused laser beam through the final aperture, depending on the position of the sample relative to the beam constriction.

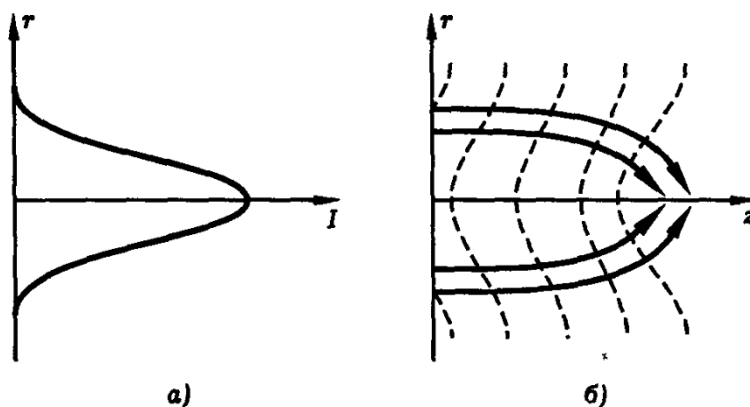


Figure 3.1 – Self-focusing of light. Intensity profile of the Gaussian light beam (a), curvature of the wave front of the Gaussian beam (dashed curves) due to the nonlinearity of the medium $n_2 > 0$ (b) [1]

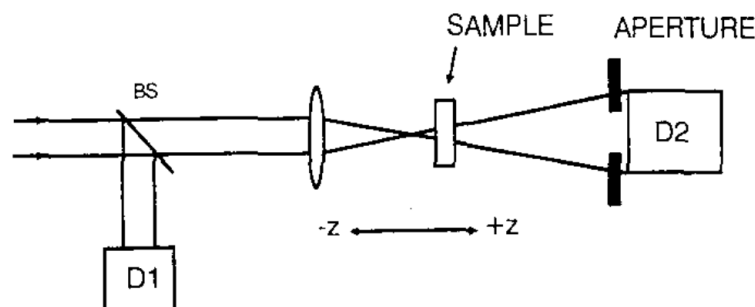


Figure 3.2 – General scheme of z-scan installation [2]

Consider a sample with a positive nonlinear addition to the refractive index, the thickness of which is less than the diffraction length of the beam. In this case, we can take it as a thin lens, the optical power of which changes as it moves along the optical axis of the system. We start with the position before the focus (z is negative) – here the radiation intensity is relatively small, i.e. nonlinear refraction can be ignored, and therefore the transmission of the aperture remains unchanged. As the sample gets closer to the focus, the radiation intensity in it increases, which leads to self-focusing. The appearance of an induced collecting lens before the beam focus leads to an increase in its divergence after the focus. Consequently, the transmission of the aperture is reduced. Gradually, the sample passes the bundle constriction, appearing to be to its right (z is positive). Here, on the contrary, self-focusing of radiation leads to a decrease in the divergence of the beam, which is expressed in its narrowing, and an increase in the transmission of the aperture.

The presence of a minimum transmission followed by a transition to the maximum indicates a positive n_2 of the medium. Negative n_2 , by analogy, is

expressed in the opposite arrangement of the minimum and maximum transmittance.

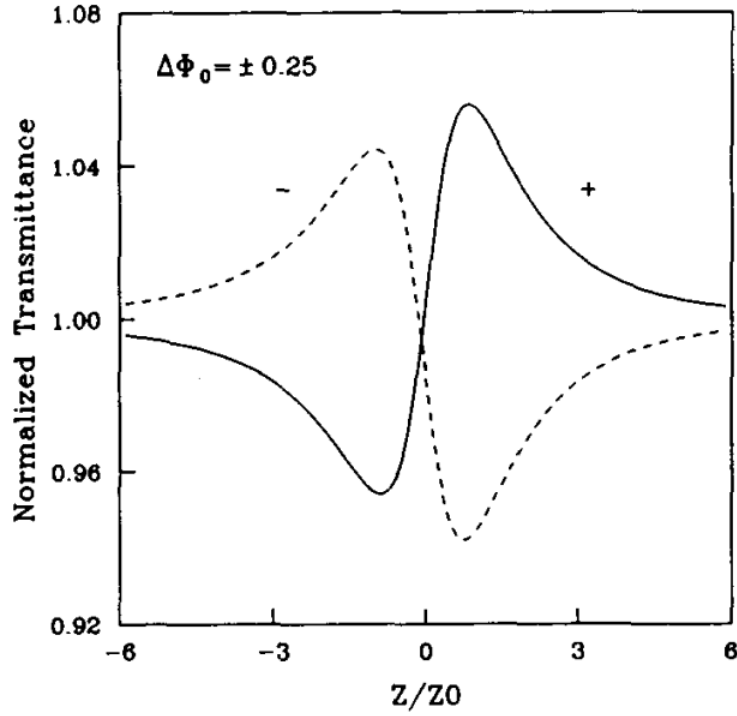


Figure 3.3 – Typical z-scan curves for samples with positive (solid line) and negative (dashed line) n_2 [2]

It should be noted that the above description does not take into account the presence of nonlinear absorption in the sample. The sensitivity of the technique to nonlinear refraction is due solely to the presence of an aperture, and its removal will make it impossible to observe this effect. However, in this case, the z-scan will still be sensitive to nonlinear absorption. In this way, the combination of closed-and open-aperture measurements allowed us to obtain both nonlinear absorption and nonlinear refraction coefficients separately. If these effects are present at the same time, the curve obtained with a closed aperture should be normalized to the results of measurements with an open aperture.

The sample transmission difference (z-scan curve difference) can be expressed as:

$$\Delta T = 0,406(1 - S)^{0.25} \left| \frac{\omega}{c} n_2 I L_{eff} \right|, \quad (3.5)$$

where $L_{eff} = (1 - e^{-\alpha L})/\alpha$ is the effective thickness of the sample, α is the linear absorption coefficient, S is the transmission of the aperture in the absence of nonlinear effects, and I is the radiation intensity in the beam constriction. From this, we obtain an expression for calculating n_2 based on the z-scan curve:

$$n_2 = \frac{\Delta T}{0,406(1 - S)^{0,25} I L_{eff}} \cdot \frac{c}{\omega}. \quad (3.6)$$

The radiation intensity is calculated based on the assumption that the beam is Gaussian, that is, its pre-stretch radius is calculated using the formula:

$$r_0 = \frac{4\lambda f}{\pi D}, \quad (3.7)$$

where λ is the radiation wavelength, D is the initial beam diameter, and f is the focal length of the lens. Then the intensity of radiation with power P will take the form:

$$I = \frac{P}{\pi r_0^2}. \quad (3.8)$$

DESCRIPTION OF THE EXPERIMENTAL SETUP

An Ytterbium femtosecond laser with a central wavelength of 1050 nm is used as the radiation source. The characteristic integrated radiation power is 2.5 W, the pulse repetition rate is 70 MHz, and the pulse duration is 100 fs.

This experimental setup is shown in figure 3.4. Laser radiation is focused by a long-focus L_1 and passes through the sample O , fixed on a mechanized slide. On a beam-splitting plate BS the bundle is split into two parts. One hits the power meter PM_O and is used to obtain an open-aperture z-scan curve. The second one passes through L_2 , aperture A and is recorded on the power meter PM_C producing a closed-aperture z-scan curve. The short-focus lens L_2 is necessary to increase the sensitivity of the device.

INSTRUCTIONS

1. Following the lecturer's instructions, form the initial adjustment of the z-scan setup according to the diagram shown in Figure 3.4.
2. Use a micrometer to find the thickness of the sample L . Determine its linear transmission. To do this, measure the laser radiation power before and after the sample. Based on the transmission, calculate the linear absorption coefficient α .

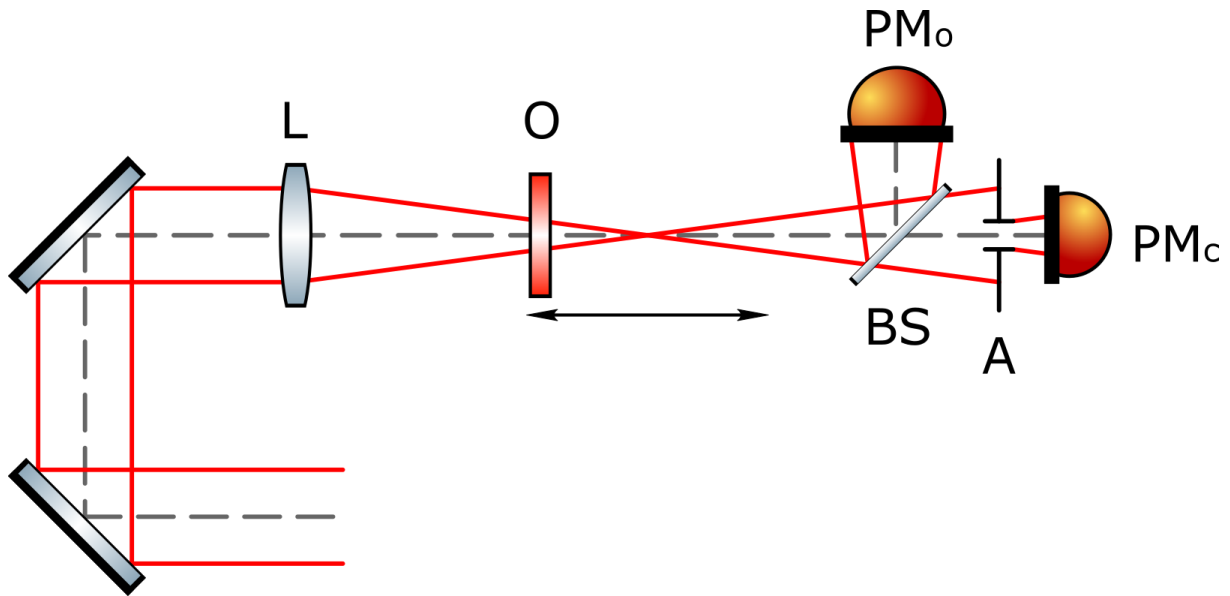


Figure 3.4 – Diagram of the experimental z-scanning setup

3. Determine the radiation intensity in the constriction. To determine its geometric parameters, it is necessary to measure the beam width in front of the lens, as well as its focal length. Measure the radiation power immediately after the lens to avoid damage to the detection head.
4. Set the sample on a motorized slide, orient it normally to the laser beam.
5. Measure the transmission of the aperture S , in the absence of nonlinear effects, i.e., when the sample is far from the beam constriction.
6. By shifting the sample relative to the constriction using a motorized slide, obtain the z-scan curve for cases with an open and closed aperture.
7. Determine the nonlinear refractive index coefficient of the material under study

SELF-ASSESSMENT QUESTIONS

1. In what media is it possible to observe third-order nonlinear effects?
2. Give some examples of effects resulting from cubic nonlinearity. Describe concisely the essence of one of them (except for self-focusing).
3. What causes the effect of self-focusing of beams with a Gaussian intensity profile? How will a beam with a rectangular intensity distribution behave in a nonlinear medium?

4. What is the difference between open and closed aperture z-scan measurements, and what are their results of measurements?

References

- [1] Akhmanov S. A., Nikitin S. Yu. Physical optics. Textbook— - 2004.
- [2] Sheik-Bahae M. et al. Sensitive measurement of optical nonlinearities using a single beam // *IEEE Journal of Quantum Electronics*. – 1990. – T. 26. – №. 4. – C. 760-769

Laboratory assignment №4

TERAHERTZ TIME-DOMAIN SPECTROSCOPY

Work objective:

To study the principle of operation of a terahertz (THz) spectrometer with time resolution and to measure the transmission spectrum, as well as the refractive index and extinction coefficient of materials in the terahertz frequency range.

Tasks:

1. To get to know the operating principle and design features of a terahertz spectrometer;
2. To measure the intensity time forms of the THz pulses that have passed through the materials proposed for the study;
3. To calculate the transmission spectra of objects, as well as the values of their refractive index and extinction coefficient in the terahertz region of the spectrum.

SOME THEORY

Basics of THz optics

Terahertz (THz) radiation is electromagnetic radiation with a wavelength range from 30 microns to 3 mm or with frequencies from 0.1 to 10 THz. The terahertz band was not available for research until the 1980s, due to the lack of its effective coherent sources and receivers. With their introduction, interest in terahertz technologies began to grow rapidly, due to a number of features inherent for this frequency range.

The wide use of THz radiation is due, among other things, to the fact that many rotational and vibrational transitions of molecules correspond exactly to the frequencies under consideration. Terahertz spectroscopy allows both simple identification of chemical substances and a more detailed study of their structure. It is noteworthy that terahertz radiation has a low photon energy, that is, it is nonionizing and safe for humans. A relatively large wavelength ensures its low scattering. All this makes terahertz radiation a universal and safe tool for both medical and environmental diagnostics, as well as for security systems or wireless information transmission.

The laboratory assignment will deal with introducing the technique of terahertz spectroscopy with time resolution – a unique approach that allows you to simultaneously obtain information about both the amplitude and the phase of

radiation transmitted through the sample, and therefore comprehensively specify the optical properties of the latter.

THz radiation generation

There are many ways to generate terahertz radiation. For the first time, pulsed coherent THz radiation was generated using a special photoconductive antenna illuminated by femtosecond infrared pulses. The highest-intensity THz radiation to date is generated by optical rectification of fs pulses in organic crystals.

In the installation considered in this laboratory assignment, the generation of THz radiation occurs due to the Dembers effect in the InAs semiconductor crystal. When a semiconductor is illuminated by radiation that is effectively absorbed by this semiconductor, the formation of nonequilibrium electrons and holes occurs mainly near the surface. The generated charge carriers begin to drift from the area of higher illumination to the less illuminated area, that is, deeper into the crystal. In this case, the electrons with a significantly lower effective mass (and, as a consequence, a significantly higher diffusion coefficient) are more distant from the generation site than the holes. The spatial separation of charges leads to the formation of an electric dipole in the crystal located perpendicular to the surface. With the end of the femtosecond pulse, the generation of nonequilibrium charge carriers also ends, which leads to the collapse of the dipole. The accelerated motion of charges is accompanied by radiation, the frequency of which lies in the terahertz range.

The most powerful Dember effect occurs in semiconductors with a narrow band gap and high electron mobility, such as InAs and InSb. In addition, to increase the efficiency of THz radiation generation, semiconductor crystals are placed in a highly inductive constant magnetic field.

Electro-optical detection

The principle of electro-optical detection is based on the Pockels effect signal that is pronounced in a birefringent optical medium under the action of a constant or alternating electric field, which allows you to directly register its amplitude. This effect occurs only in crystals that do not have a center of symmetry (or in other noncentrosymmetric media). The most commonly used crystals are ZnTe, CdTe, GaP, and GaAs.

Consider the electro-optical detection system used in the laboratory setup to be described. In the absence of THz radiation, an IR probe beam passes through an electro-optical (EO) sensor and the CdTe crystal retains its original linear polarization. With the help of a quarter-wave plate, the polarization is transformed into a circular one, and its edges on the Wollaston prism are separated in space, after which they are detected using a balanced detector (DB). There, the currents generated on two photodiodes are subtracted, and the received signal is transmitted to a PC via an analog-to-digital converter. In the absence of THz

radiation, the polarization components of the probe beam are equal to each other, and the recorded signal is zero.

Next, we consider the case when terahertz radiation propagates co-directionally with the reference beam, and also focuses on the EO crystal to achieve a higher intensity in the intersection region. In this case, the terahertz field induces birefringence in the crystal, the value of which linearly depends on the amplitude of THz radiation. The resulting anisotropy leads to a phase delay between the polarization components of the probe beam, which is why its polarization is transformed from linear to elliptical in the crystal. Consequently, the intensities of the two beams coming out of the Wollaston prism are not equal to each other, and the signal of the balanced detector is nonzero. This process is shown on Figure 4.1

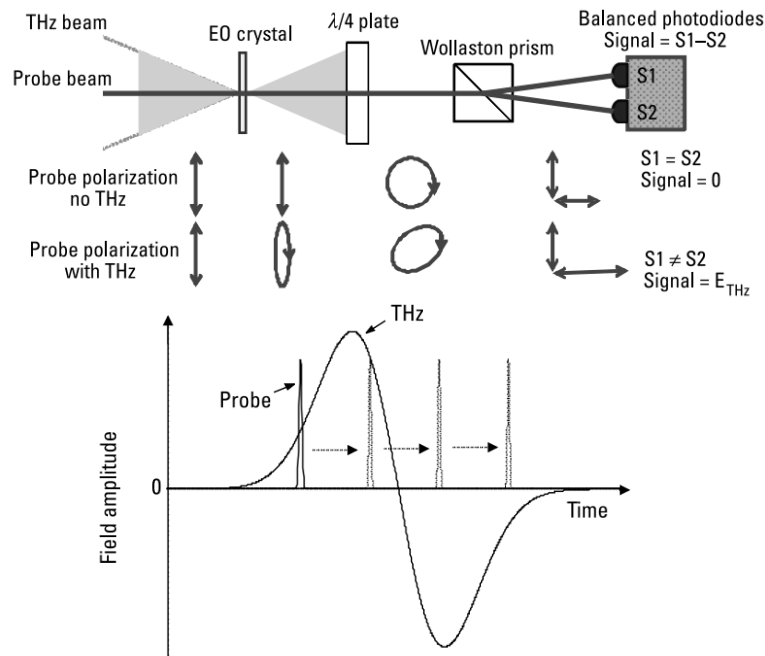


Figure 4.1 - The principle of the electro-optical detection technique

The Pockels effect method is characterized by low inertia, so the method described above allows us to resolve fast-moving processes in time. Thus, the typical duration of a THz pulse is 0.5-2 ps, and the duration of a test femtosecond pulse is about 100 fs. This fact allows us to assume that the field of a THz pulse is constant at some point in time for the entire femtosecond pulse. By shifting one pulse relative to another using a delay line, you can gate the THz pulse, that is, directly get its time form.

Data processing

The result of measurements made during terahertz spectroscopy with time resolution is the time forms of pulses. As a rule, two measurements are made: for the pulse that has passed through the sample, and for the pulse that is distributed in the absence of the sample. The first one is called object $E_{sam}(t)$, the second one is called reference $E_{ref}(t)$. Further, the received signals are converted from the time domain to the spectral domain using the Fourier transform. The corresponding spectra are denoted by $E_{sam}(\omega)$ and $E_{ref}(\omega)$.

The spectrum of a pulse transmitted through a plane-parallel dielectric plate has the form:

$$E_{sam}(\omega) = \frac{4\hat{n}_s n_0}{(\hat{n}_s + n_0)^2} \exp\left[-i\hat{n}_s \frac{\omega l}{c}\right] \cdot E_0(\omega), \quad (4.1)$$

where $\hat{n}_s = n_s - ik_s$ is the complex refractive index of the sample, n_0 is the refractive index of the surrounding medium (in the simplest case, air), and l is the radiation propagation length in the sample, which is equal to its thickness at the normal angle of incidence. The corresponding reference spectrum is measured under similar conditions, but in the absence of a sample:

$$E_{sam}(\omega) = \exp\left[-in_0 \frac{\omega l}{c}\right] \cdot E_0(\omega). \quad (4.2)$$

Extracting the optical characteristics of a sample requires calculating its transfer function:

$$H_0(\omega) = \frac{E_{sam}(\omega)}{E_{ref}(\omega)} = \frac{4\hat{n}_s n_0}{(\hat{n}_s + n_0)^2} \exp\left[-k_s \frac{\omega l}{c}\right] \exp\left[-i(n_s - n_0) \frac{\omega l}{c}\right]. \quad (4.3)$$

Often, the refractive $\widehat{index} n(\omega)$ is used, which is included in the Fresnel transmission coefficient (i.e., in the first multiplier), is approximated only by the real part of n_s :

$$H(\omega) = \frac{4n_s n_0}{(n_s + n_0)^2} \exp\left[-k_s \frac{\omega l}{c}\right] \exp\left[-i(n_s - n_0) \frac{\omega l}{c}\right]. \quad (4.4)$$

Taking the argument and the logarithm of the simplified transfer function produces, respectively:

$$\angle H(\omega) = -i(n_s - n_0) \frac{\omega l}{c}, \quad (4.5)$$

$$\ln|H(\omega)| = \ln \left[\frac{4n_s n_0}{(n_s + n_0)^2} \right] - k_s \frac{\omega l}{c}. \quad (4.6)$$

From equation (4.5)-(4.6), the refractive index and extinction coefficient can be calculated:

$$n_s = n_0 - \frac{c}{\omega l} \angle H(\omega), \quad (4.7)$$

$$k_s = \frac{c}{\omega l} \left\{ \ln \left[\frac{4n_s n_0}{(n_s + n_0)^2} \right] - \ln|H(\omega)| \right\}. \quad (4.8)$$

The transfer function $H(\omega)$ is derived from the experimental data obtained during the measurement of the object and the reference signals.

In addition, it is important to note that the above reasoning does not take into account the presence of the Fabry-Perot effect – multiple reflections of radiation from the sample faces, and the subsequent occurrence of secondary pulses in the signal. However, if the plane-parallel plate is sufficiently thick, the secondary pulses lag behind the signal by a time greater than their duration, which allows them to be removed from the signal by applying a time window. One of the functions used for this purpose is the Supergauss function:

$$sg(t) = \exp \left[- \left(\frac{(t - t_0)^2}{2\sigma^2} \right)^p \right], \quad (4.9)$$

where $t_0 = \frac{t_{max} + t_{min}}{2}$ defines the position of the window function, and $\sigma = \frac{t_{max} - t_{min}}{2}$ defines its width. The exponent p is responsible for the rate of decline of the function at the edges, it can be assumed to be equal to 20.

DESCRIPTION OF THE EXPERIMENTAL SETUP

Experimental setup

An Ytterbium femtosecond laser with a central wavelength of 1050 nm is used as the radiation source. The characteristic integrated radiation power is 2.5 W, the pulse repetition rate is 70 MHz, and the pulse duration is 100 fs.

A diagram of a time-resolved terahertz spectrometer is shown in Figure 4.2. The femtosecond laser radiation is separated by a beam splitter BS into the test beam and the pump beam. The pump beam is modulated by an opto-mechanical interrupter M , passes the optical delay line and hits the terahertz generator G . The latter is a semiconductor indium arsenide crystal InA placed in a magnetic field with an induction of 2.4T. The generated THz radiation passes through a Teflon

filter TF , which absorbs the pump radiation reflected from the semiconductor crystal. The lens L_1 collimates the beam, and L_2 focuses it on the object under study. The transmitted THz radiation is again collimated by the lens L_3 and fed into the electro optical detection system using a parabolic mirror PM . Synchronous amplifier SA is used to increase the useful signal-to-noise ratio. After that, the signal is digitized by an analog-to-digital converter and recorded using special software on PC.

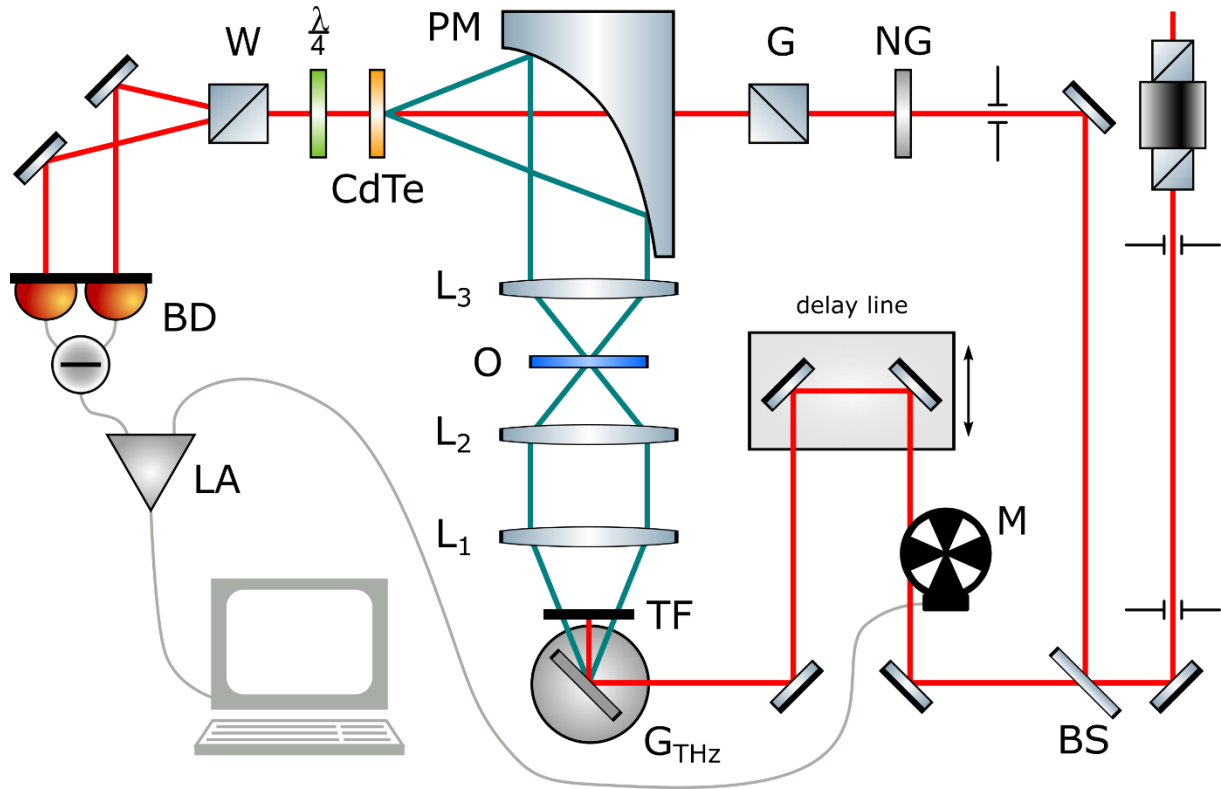


Figure 4.2 - Diagram of a terahertz spectrometer with time resolution

Working with experimental layout management software

Two programs are used to control the THz spectrometer: *Measure* and *TDS_Discrete*

Measure - allows you to perform initial signal removal and quickly manage the optical delay line. Used at the preparatory stage of work.

Operation algorithm:

1. Launch the program by clicking the corresponding buttons in the upper-left corner.



2. Create, at the program's request, a text file in which the recorded signal values will be saved.
3. Click the *Find devices*, button to connect the PC to the equipment used in the experimental setup.
4. In the field *Movement*, set the step of movement and the speed of its movement. *Step* is always 1/8; speed: for fast movement without removing the signal use 500, for rough removal of the signal use 100, for accurate removal use 30.
5. In the *Destination Position* field, specify the destination point in the progress steps. In this case, the current position of the slide is displayed in the *Current Position* field.
6. To start moving, press the *Start* button, and then the *Stop*. If you need to change the speed or direction of the movement, you first stop it with the button *Stop*, and then change the parameters!
7. Click the *Stop* button in the upper-left corner to finish your work.

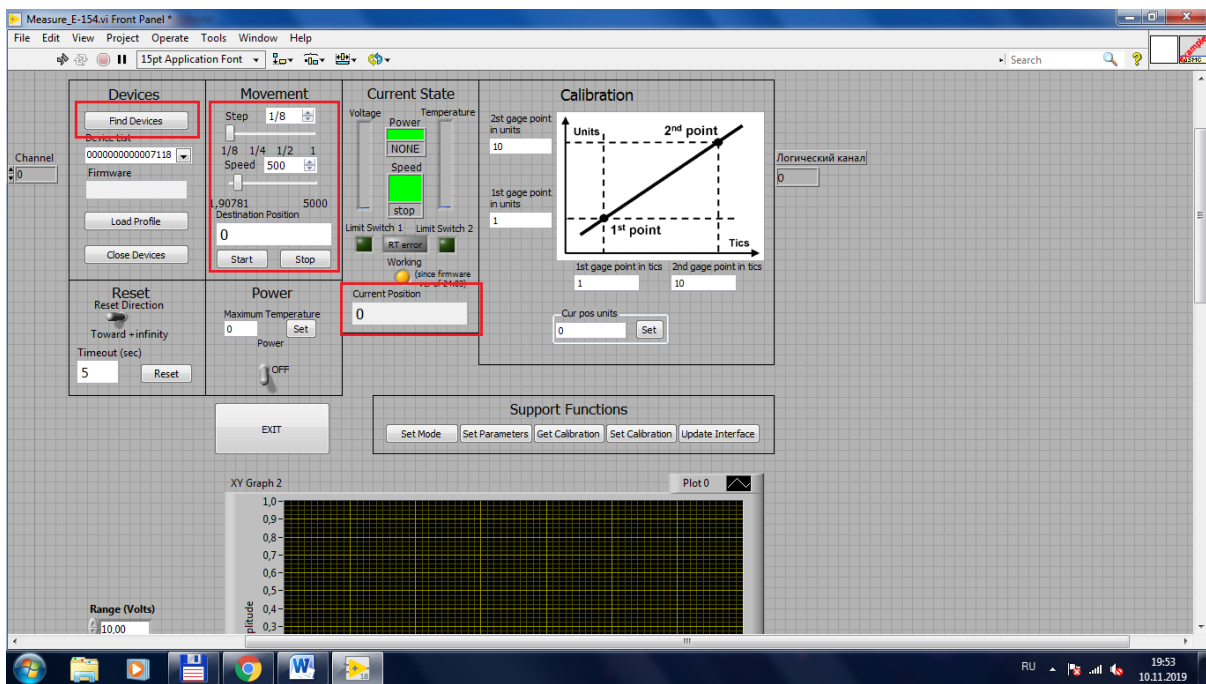


Figure 4.3 -*Measure* Program Interface

TDS_Discrete - used for point-by-point sampling of the signal with averaging over several dimensions. The data obtained in this program is used to obtain the optical characteristics of the objects under study.

Algorithm works:

1. Before you start working *Path*, specify the path to the folder where the data will be saved in the *Path* field.
2. Also, before starting the program, set the parameters of the recorded signal: in the *Start* field, specify the starting point (0 ps), in the *Delay* field - the signal duration in picoseconds (100 ps), in the step field - the measurement step in ps (0.2 ps), and in the *Number of samples per channel* field – the number of measurements, by which the signal will be averaged (30 measurements).
3. Launch the program by clicking the corresponding buttons in the upper-left corner.



4. When the program is finished, it will automatically stop.

As a result of the program, text files will be created in the specified folder, where the values of the THz field strength in relative units will be recorded for each time step. The number of files corresponds to the number of dimensions over which the signal is averaged. Additionally, a file will be created with the name *Average_[folder name]*, where the average signal values will be shown. It is used in the further processing of experimental data.

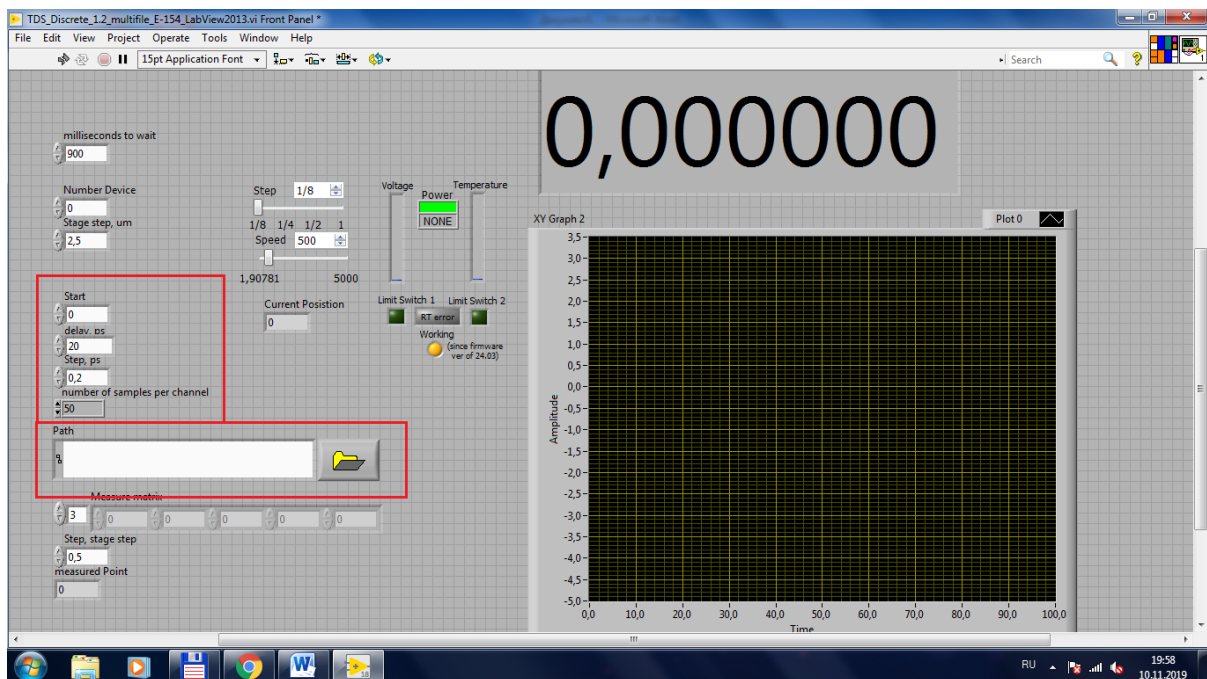


Figure 4.4 - TDS_Discrete program interface

INSTRUCTIONS

1. Strictly according to the teacher's instructions, perform the initial adjustment of the terahertz spectrometer with time resolution according to the scheme shown in Figure 4.2.
2. On the PC, run the program for removing data from the laboratory layout. Measure the THz pulse field in the absence of a sample (reference signal).
3. While this measurement is on, measure the thickness of the test sample using a micrometer.
4. Block the input of laser radiation to the detection system, remove the TF filter from the optical circuit. Place the object under study in the constriction of the THz beam, guided by the glare of IR radiation reflected from the surface of the crystal generator. Set the *TF* filter back.
5. Measure the field of the THz pulse having passed through the sample (subject signal).
6. Perform processing of experimental data, according to the information provided in the manual. If there are re-reflections in the signal, remove them using the super-Gaussian function.
7. Plot the time forms and spectra of the THz pulses obtained during the experiment, as well as the dependencies of the transmission of the sample, its refractive index, and the extinction coefficient in the terahertz frequency range.

SELF-ASSESSMENT QUESTIONS

1. What mechanism explains the increase in the efficiency of THz radiation generation in an InAs crystal due to the application of an external magnetic field?
2. What is the limitation of the resolution of the temporal shape of the THz pulse recorded by the method of electro-optical detection?
3. Is it possible to measure the optical properties of layered materials using THz spectroscopy with time resolution? For example, a layer of paint applied to a polymer substrate.
4. How will presence of multiple re-reflections from the sample faces in the time form of THz signal affect the emission spectra? How can we avoid this influence?

References

- [1] Zhang X. C., Xu J. Introduction to THz wave photonics. – New York: Springer, 2010. – T. 29. – P.246.
- [2] Naftaly M. Terahertz metrology. – Artech House, 2015.
- [3] Klatt G. et al. Terahertz emission from lateral photo-Dember currents //Optics express. – 2010. – T. 18. – №. 5. – C. 4939-4947.
- [4] Bespalov V. G. et al. Methods of generating superbroadband terahertz pulses with femtosecond lasers //Journal of Optical Technology. 2008, vol.75, no. 10, pp. 636-642.

Набилкова Александра Олеговна

Опарин Егор Николаевич

Цыпкин Антон Николаевич

**LABORATORY ASSIGNMENTS FOR
THE COURSES OF "FEMTOSECOND OPTICS AND
FEMTOTECHNOLOGY"
AND "TERAHERTZ TECHNOLOGIES"
(Experimental part)**

Учебно-методическое пособие

В авторской редакции

Редакционно-издательский отдел Университета ИТМО

Зав. РИО

Н.Ф. Гусарова

Подписано к печати

Заказ №

Тираж

Отпечатано на ризографе